High performance feedback for fast scanning atomic force microscopes

G. Schitter
Nanotechnology Group, Swiss Federal Institute of Technology, ETH Center CLA, CH-8092 Zürich, Switzerland

P. Menold
Institute for Systems Theory in Engineering, University of Stuttgart, Pfaffenwaldring 9, D-70569 Stuttgart, Germany

H. F. Knapp[a)]
Nanotechnology Group, Swiss Federal Institute of Technology, ETH Center CLA, CH-8092 Zürich, Switzerland

F. Allgöwer[b)]
Institute for Systems Theory in Engineering, University of Stuttgart, Pfaffenwaldring 9, D-70569 Stuttgart, Germany

A. Stemmer[c)]
Nanotechnology Group, Swiss Federal Institute of Technology, ETH Center CLA, CH-8092 Zürich, Switzerland

(Received 20 February 2001; accepted for publication 4 June 2001)

We identify the dynamics of an atomic force microscope (AFM) in order to design a feedback controller that enables faster image acquisition at reduced imaging error compared to the now generally employed proportional integral differential (PID) controllers. First, a force model for the tip–sample interaction in an AFM is used to show that the dynamic behavior of the cantilever working in contact mode can be neglected for control purposes due to the relatively small oscillation amplitude of the cantilever in response to a defined topography step. Consequently, the dynamic behavior of the AFM system can be reduced to the behavior of the piezoelectric scanner making the design of a model based controller for the AFM possible. Second, a black box identification of the scanner of a commercial AFM (Nanoscope IIIa, Digital Instruments) is performed using subspace methods. Identification yields a mathematical model of the scanner which allows us to design a new controller utilizing H_∞ theory. Finally, this controller is implemented on an existing AFM and operated in contact mode. We demonstrate that such an H_∞-controlled AFM system, while scanning at rates five times faster than conventional PID-controlled systems, operates with reduced measurement error and allows scanning at lower forces. © *2001 American Institute of Physics.* [DOI: 10.1063/1.1387253]

I. INTRODUCTION

Atomic force microscopes (AFM) use a sharp tip supported on a cantilever to trace the topography of a sample scanned underneath the tip by a piezoelectric scanner (Fig. 1). In the so-called contact mode, the deflection of the cantilever is often monitored by an optical lever and a segmented photodiode. Generally, a proportional integral differential (PID)-feedback scheme is employed to keep the deflection of the cantilever, and thus the imaging force, constant by varying the position of the sample along the z axis according to its topography. The actual value of the imaging force can be set by the setpoint. This operation mode is referred to as the ''constant force mode.'' Although the atomic force microscope is capable of imaging surface features at high resolution, it only does so at relatively low speeds. Larger images at the micrometer scale, which are usually taken in the constant force mode to avoid damage to sample and tip, can take several minutes to acquire. This is mostly due to the low resonant frequency of the piezoelectric scanners used for scanning and responding to the PID-feedback signal controlling the imaging force. Faster scan speeds will result either in oscillations of the scanner or, if the PID-feedback settings are set low enough to avoid such oscillations, an increase in the cantilever deflections around the setpoint value. Both situations lead to variations of the imaging force which might damage the sample and/or tip. Furthermore, in the former case, images will be distorted by oscillations caused by instabilities of the closed loop AFM system consisting of the scanner, the cantilever, the photodiode, and the controller system. Several approaches have been taken to enable faster image acquisition. The easiest method is to scan in the constant height mode, i.e., to disable the feedback completely.[1,2] This, of course, introduces the problem of varying force as mentioned above. A method devising a special feedback strategy to compromise between constant

[a)]Present address: CSEM Alpnach, Untere Gründlistrasse 1, CH-6055 Alpnach, Switzerland.
[b)]Corresponding author; electronic mail: allgower@ist.uni-stuttgart.de
[c)]Corresponding author; electronic mail: stemmer@nano.mavt.ethz.ch

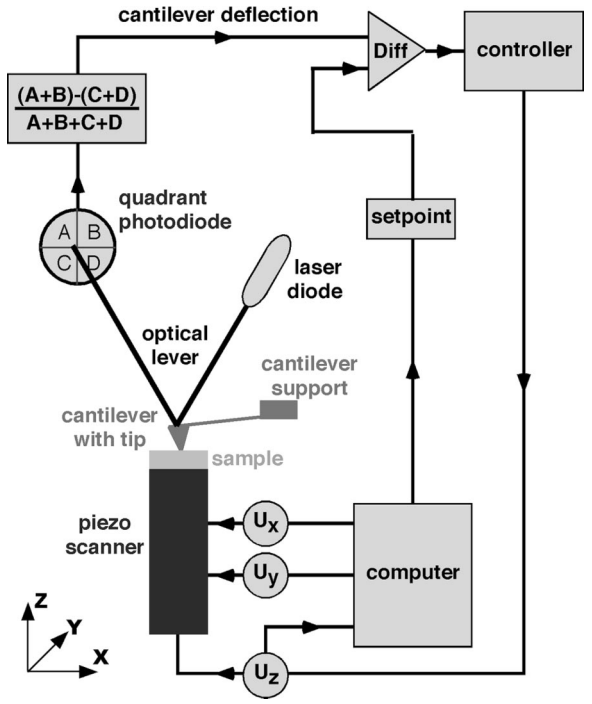

FIG. 1. A schematic diagram of an atomic force microscope.

height and constant force mode has also been implemented,[3] which ameliorates the force problem to some extent. Other approaches circumvent the low resonance frequency of the scanner by either introducing high frequency piezo segments to the scanner for its z movement[4–7] or by employing cantilever arrays with integrated actuators allowing direct force control through the cantilever and imaging in parallel.[8,9] The former approach limits the z range and the maximum sample height whereas the latter requires specially designed cantilevers. Finally, there is the approach of using better feedback strategies for the AFM system which is pursued in this article. To our knowledge, only theoretical investigations in this direction have been published that are concerned with the cantilever-sample interaction[10,11] or the scanner.[12]

This article presents both the mathematical modeling of the complete AFM system as well as the design and implementation of a new controller. The main interest is to increase the scanning rate by utilizing model based modern control methods. The controller, which is designed for high performance, has to be robust because of the nonlinearities of the system and the uncertainties of the model.

To design a robust controller, a mathematical model of the atomic force microscope is required.[13] Therefore the individual system components which are part of the closed loop controlled AFM system have to be modeled. These components are the tip–sample interactions, the cantilever, the photodiode, and the piezo scanner. The input of the scanner's z-voltage amplifier is regarded as input of the AFM system. The output of the AFM system is the signal of the photodiode.

In Sec. II of this article two physical models are derived. The first physical model concerns the tip–sample interaction, which is based on the Johnson–Kendall–Roberts (JKR) force model,[15] while the second model describes the dynamic behavior of the cantilever.[14,15]

TABLE I. Parameters of the JKR force model.

R	radius of the tip
ρ_1	number density of the tip
ρ_2	number density of the sample
ϵ	minimum energy of the Lennard-Jones potential
σ	spherical approximation of the molecule diameter

The third section presents a black box identification[16] of the piezo scanner using subspace methods[17,18] to obtain the mathematical model of the scanner dynamics in the z direction, which is along the axis of symmetry of the piezoelectric scanner.

Finally, in the fourth section an H_∞ controller,[13] which considers the higher frequency dynamics of the closed-loop AFM system, is designed for the purpose of accelerating the scanning process in constant force mode. The designed controller is subsequently implemented on an existing AFM operating in contact mode.

Experiments compare a well-tuned PID controller, which is implemented on our commercial AFM system, with the derived H_∞ controller (Sec. V) and show that a significant improvement in scanning speed can be achieved without having to compromise resolution.

II. PHYSICAL MODELING

A. Tip–sample interaction

For scanning of hard samples, the JKR force model can be used which considers only interactions in the contact area between tip and sample.[14,15] This model consists of the Lennard-Jones potential and a modified Hertz model. The force interaction of the Lennard-Jones type

$$F(z)=f_0R\left[-\left(\frac{\sigma}{z}\right)^2+\frac{1}{30}\left(\frac{\sigma}{z}\right)^8\right] \tag{1}$$

is composed of the attractive Van der Waals interaction

$$-f_0R\left(\frac{\sigma}{z}\right)^2 \tag{2}$$

and the strong repulsive force which is attributed to the Pauli principle

$$f_0R\,\frac{1}{30}\left(\frac{\sigma}{z}\right)^8, \tag{3}$$

with

$$f_0=\tfrac{2}{3}\pi^2\epsilon\rho_1\rho_2\sigma^4 \tag{4}$$

and the tip–sample separation z. The parameters of this model are summarized in Table I.

The Hertz model describes the interaction between two spheres and considers the deformation of the spheres, if they are in contact. By setting the radius of the sample to infinity we get the interaction between a plane surface and a spherical tip. This model has to be modified because the zero point

TABLE II. Parameters of the modified Hertz model.

z_0	zero point of the Lennard-Jones potential
ν_1	Poisson ratio of the tip
ν_2	Poisson ratio of the sample
E_1	Young's modulus of the tip
E_2	Young's modulus of the sample

of the resulting force has to be identical with the zero point of the Lennard-Jones potential z_0.[15] Assuming a small indentation of the plane by $|z_0-z| \ll R$ we get

$$F(z)=g_0(z_0-z)^{3/2}, \tag{5}$$

with

$$g_0=\frac{8\sqrt{2}}{3\pi\left(\frac{1-\nu_1^2}{\pi E_1}+\frac{1-\nu_2^2}{\pi E_2}\right)}\sqrt{R}, \tag{6}$$

where the parameters are described in Table II. Combining these two force models we get

$$F(z)=\begin{cases} f_0 R\left[-\left(\frac{\sigma}{z}\right)^2+\frac{1}{30}\left(\frac{\sigma}{z}\right)^8\right] & \text{if } z>z_0 \\ g_0(z_0-z)^{3/2} & \text{if } z\leqslant z_0 \end{cases} \tag{7}$$

and the force curve shown in Fig. 2.

B. Cantilever dynamics

By exciting the cantilever with a sinusoidal sweep signal, we see that the spectrum of the cantilever shows just one main resonance frequency (Fig. 3). Thus the cantilever can be modeled as a soft damped single spring mass resonator, which is detuned by the nonlinear force $F(z)$ given by Eq. (7). The equations of motion of the oscillator system are

$$\begin{aligned} \dot{d}_1(t)&=d_2(t), \\ \dot{d}_2(t)&=-\frac{\omega_0}{Q}d_2(t)-\frac{k}{m}[d_1(t)-z_1]+\frac{1}{m}F(d_1(t)), \end{aligned} \tag{8}$$

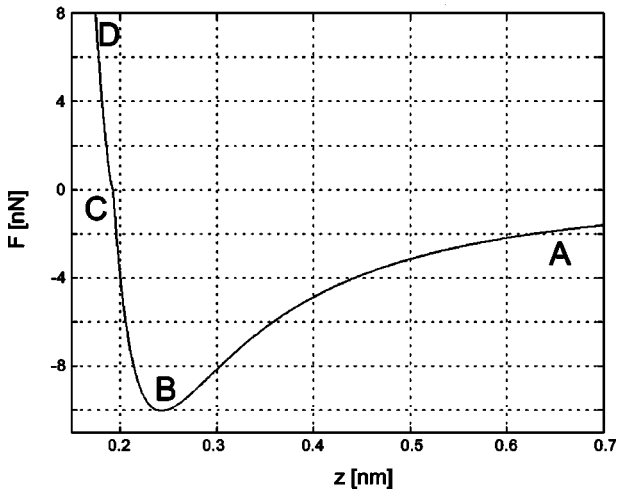

FIG. 2. The force F as a function of the tip–sample separation z. Section AC shows the Lennard-Jones potential. In section AB the Van der Waals interaction dominates and in section BC the Pauli repulsion dominates. Section CD shows the modified Hertz model.

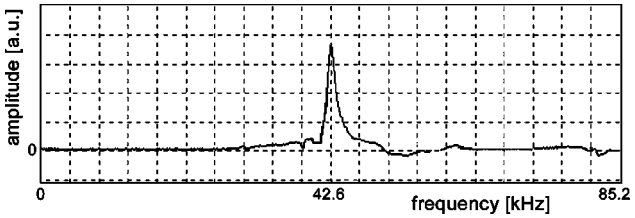

FIG. 3. Amplitude spectrum of the cantilever used in the identification of the scanner.

with the position d_1 and the velocity d_2 of the tip. The variables used in Eq. (8) are described in Table III. This model describes the oscillation of the cantilever above a flat surface. For consideration of the sample's topography the model has to be extended by an input u. Due to the scanning process this new model input u is a function of time. Transforming Eq. (8) into a new state space model by using the coordinates and the system input u and output w as shown in Fig. 4 we get

$$\begin{aligned} \dot{d}_1(t)&=d_2(t), \\ \dot{d}_2(t)&=-\frac{\omega_0}{Q}d_2(t)-\frac{k}{m}[d_1(t)-z_1+u(t)]+\frac{1}{m}F(d_1(t)), \\ w(t)&=-d_1(t)+u(t), \end{aligned} \tag{9}$$

with the topography $u(t)$ of the sample.

C. Simulation of contact mode

Figure 5 shows the time response of the deflection to a step up and step down in the sample surface simulating Eq. (9) and the behavior of the force $F(d_1(t))$. The simulated steps have a height of 1 nm [Fig. 5(a)]. The parameter values used for the simulation are shown in Table IV.

The spring constant of the cantilever is calculated by measuring its dimensions with a scanning electron microscope and using the equation presented by Sader.[21] The quality of the oscillator is defined by the equation

$$Q=\frac{\omega_0}{\Delta\omega}, \tag{10}$$

with the resonance frequency ω_0 of the cantilever and the bandwidth $\Delta\omega$ at $1/\sqrt{2}$ of the resonance peak height. The mass of the cantilever is reduced to its free end[14] and is calculated by the equation

$$m=\frac{k}{\omega_0^2}. \tag{11}$$

The nonlinear nature of the tip–sample interaction as shown in Fig. 2 can be seen in the asymmetrical response

TABLE III. Variables of the equation of motion of the cantilever.

$F(d_1)$	interaction force
Q	quality factor of the oscillating cantilever
ω_0	resonance frequency of the cantilever
k	spring constant of the cantilever
m	reduced mass of the cantilever
z_1	static height of the tip

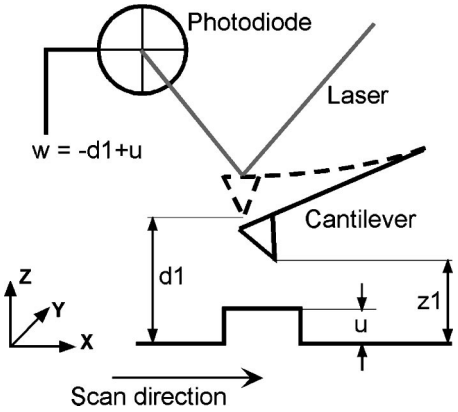

FIG. 4. Schematic diagram of the AFM system showing the dimensioning used for the transformation of the equations of oscillation into a new state space model with the sample topography as input u and the signal of the photodiode as output w.

signal to the step up and down, respectively [Fig. 5(d)]. Figure 5(b) shows the deflection signal of the cantilever. Figure 5(c) shows a close-up of Fig. 5(b) highlighting the cantilever oscillation after the step up. Apparently, the oscillation amplitude is negligible compared to the height of the step, i.e., for the contact lever used in the simulation, the amplitude of the damped oscillation as a result of the tip–sample interaction is only a tiny fraction of the deflection. For real AFM systems, the magnitude of this oscillation is usually below the precision of the analog-to-digital converter. Furthermore, the frequency of the oscillation is in the range of 700 kHz which is beyond the dynamic range of the controller running at a sampling rate of 65 kHz.[22] Thus the dynamic behavior of the cantilever does not have to be considered and modeling

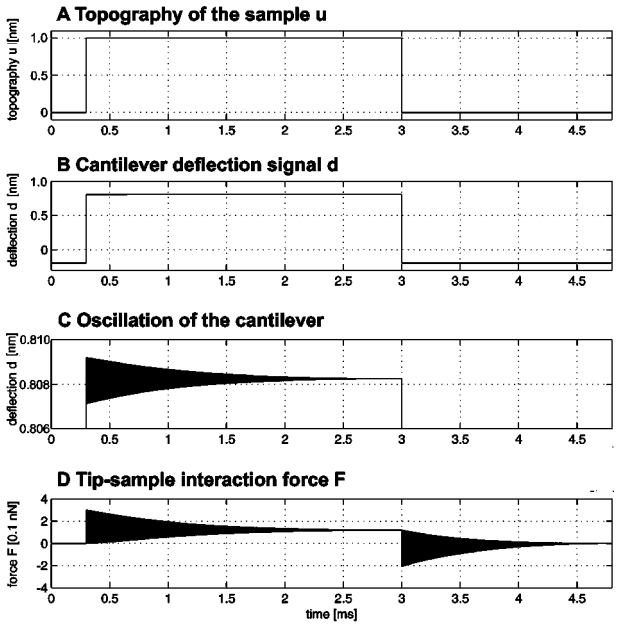

FIG. 5. Simulated response of the AFM system operating in contact mode to a 1 nm step up and down. (a) Simulated input steps. (b) Cantilever deflection signal in response to (a). (c) Close up of (b) highlighting the small oscillations of the cantilever. (d) Tip–sample interaction force in response to the input in (a). The cantilever and force oscillation wavelengths are not resolved at the time scale of this image and, thus, they are represented by their filled envelopes.

TABLE IV. Values of the parameters used in the simulation of the contact mode.

k	$0.12\ \mathrm{N\,m^{-1}}$
σ (Ref. 19)	0.34 nm
ϵ (Ref. 19)	3.79×10^{-22} J
ρ_1[a]	$5\times10^{28}\ \mathrm{m^{-3}}$
ρ_2[a]	$5\times10^{28}\ \mathrm{m^{-3}}$
R[b]	50 nm
Q[b]	100
ω_0[b]	$2\pi\times20\times10^{3}\ \mathrm{s^{-1}}$
ν_1 (Ref. 15)	0.5
ν_2 (Ref. 15)	0.5
E_1 (Ref. 14)	$179\times10^{9}\ \mathrm{N\,m^{-2}}$
E_2 (Ref. 14)	$179\times10^{9}\ \mathrm{N\,m^{-2}}$

[a]Calculated using data from Ref. 20.
[b]Parameters chosen by us, reflecting a cantilever used in the experiments.

the AFM system can be reduced to the dynamics of the piezo scanner and the photodiode. In the expected frequency and deflection range the photodiode shows a static and linear behavior and consequently can be modeled by using a constant gain. As a result, only the dynamics of the scanner have to be taken into account. Due to the complexity of the scanner, we chose to identify the scanner (see Sec. III) instead of modeling it.

III. IDENTIFICATION OF THE PIEZO SCANNER DYNAMICS

Physical modeling of the piezo scanner would be too complex because of the complex geometry and due to the fact that the scanner is a distributed system. In contrast, system identification allows one to build mathematical models of a static or dynamic system based on measured data without any need for knowledge of the system's geometry and material properties. Measured data consist of the excitation signal connected to the system's input and the system's output response to this input. For example, to identify a dynamic system consisting of a series-resonant circuit, one would connect a dynamic voltage signal to the curcuit's input and measure the voltage signal, e.g., of the capacitor. Calculating the relation between the system's input and output, one obtains the second-order differential equation describing the behavior of the resonant circuit.

To obtain the input and output data, the system is excited, e.g., by a white-noise signal, while the system's input and output signals are measured.[16] Using the measured input/output data, a mathematical model of the system is derived by utilizing several identification algorithms such as output error[16] or subspace-based[17,18] methods. The quality of the obtained model can be tested by a comparison of the model's output to the measured output using validation data which were not used for the model identification.

A. Equipment

Tests are performed on an AFM system (Nanoscope IIIa, Digital Instruments) to identify a Digital Instrument's "J" class piezoelectric tube scanner. The measurement setup for obtaining the input and output data is shown in Fig. 6. For generating the excitation a Pentium 233 MHz MMX with a CIO-DAS1601/12-A/D-D/A card (ComputerBoards) is used

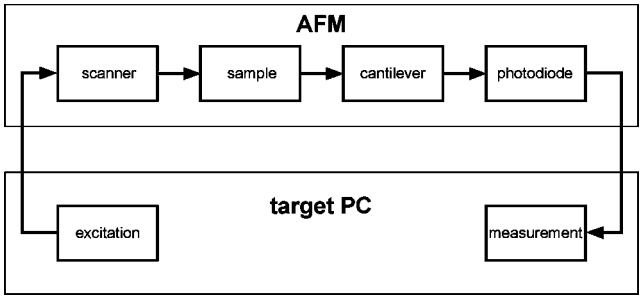

FIG. 6. Block diagram of the measurement circuit to get the input and output data for the identification of the scanner.

as the target PC operating with the Matlab Realtime Workshop.[23] The low voltage excitation signal is a bandlimited white-noise signal generated with the ''white noise block'' of Matlab Simulink, with a bandwidth of 20 kHz and several values of the noise power by varying the maximum signal amplitude from 100 to 600 mV. This signal is connected to the *z* input of the scanner's voltage amplifier. Mica is used as the sample because of its hard surface and the ability to avoid surface contamination by cleaving the sample just before each measurement. The extension and contraction of the scanner in *z* direction are measured with the usual AFM deflection measurement setup using a hard contact lever (NP Silicon Nitride Probes Nonsharpend, 100 Wide, Digital Instruments). Because the resonance frequency of this cantilever is at about 42 kHz (see Fig. 3), the dynamics of the lever should not be visible in the model. The deflection of the cantilever is measured by the photodiode whose signal is stored by the target PC.

B. System identification

From the measured input and output data a linear model of the scanner, which includes the factor modeling the photodiode, can be derived by using a numerical subspace based state space system identification algorithm.[17,18]

The model order is chosen to be four because investigations showed that a higher order does not provide substantial reduction of the modeling errors but considerably increases the calculation time of the model. The higher order model would be a limiting factor in the real time application of the control process, because the order of the controller, and thus the calculation time of the control signal, would increase.

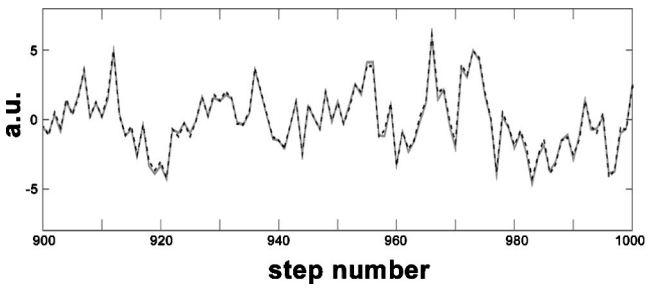

FIG. 7. Model verification of the scanner identification in the *z* direction. Comparison of the measured output (solid line) to the simulated output (dashed line) of the identified model. The two curves fit very well showing only marginal, occasional separations. The comparison was done using a separate set of validation data than the ones used for identification.

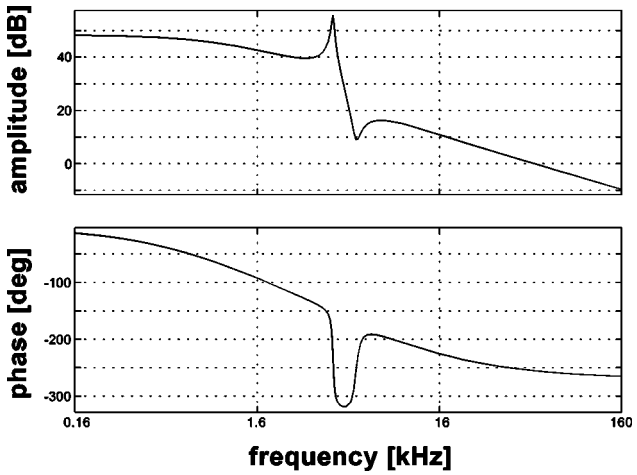

FIG. 8. Bode diagram of the identified system showing amplitude and phase of the transfer function.

Figure 7 shows a comparison of the measured output to the simulated output of the identified discrete model using validation data. It can be seen that the measurement and the simulation yield conform results and fit very well. As shown by Daniele *et al.*[12] and verified by our identification experiment (see Fig. 7), the nonlinear behavior of piezoelectric materials, i.e., hysteresis, creep, and coupling between the various motion axes, can be neglected in a first step and thus a linear model can be identified.

Figure 8 shows the bode plot of the identified system. The scanner has dominant low pass characteristics with a resonance at about 4.2 kHz and an antiresonance at about 5.5 kHz. Furthermore, the model shows two stable real poles at 1 and 3.4 kHz, respectively, and a nonminimum phase zero of the transfer function at a frequency of 9.2 kHz, which limits the possible bandwidth of the closed loop control system. Although these three values cannot be seen clearly in Fig. 8, their existence can be shown easily.[24]

PID control is sufficient for processes where the dominant dynamics are of the first or second order. For higher order processes or processes with oscillatory modes a more sophisticated control is needed to improve the performance.[25] The bandwidth of the PID-controlled AFM system is limited by the main dynamics of the scanner, which is given by a stable real pole at a frequency of about 1 kHz.

Improved control performance and, thus, faster image acquisition can be achieved using a more complex controller than the PID controller because the scanner model is of the order of four. The scanning rate can be increased by utilizing modern model based control methods because a model based controller is able to handle the high order dynamics of the system which occur at frequencies beyond the bandwidth of the PID-controlled AFM system. Another advantage of this kind of control is the robustness against model uncertainties as they could appear in a change of the deflection detection system's constant gain by using another cantilever.

IV. CONTROLLER DESIGN

Fast image acquisition is impossible using a PID controller on account of the high order dynamics of the piezoelec-

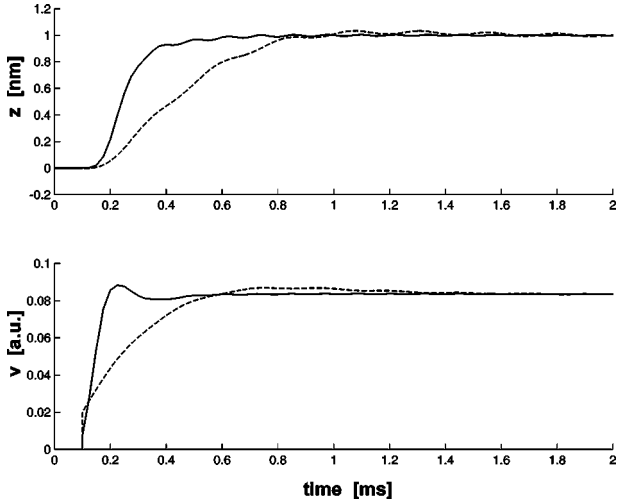

FIG. 9. Comparison of a simulated step response of the closed loop AFM system controlled by an H_∞ controller (solid line) and a well-tuned PID controller (dashed line), respectively. The upper panel shows the position z of the scanner surface and the lower panel the control signal v.

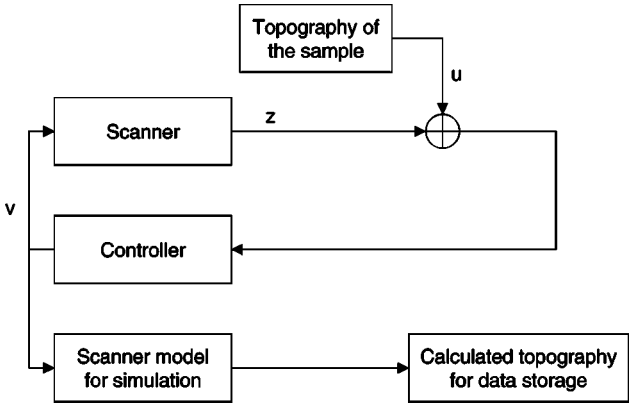

FIG. 10. Structure of the closed loop control system and the simulation of the scanner for data storage.

tric scanner (see Sec. III and Ref. 25). Control performance can be improved using modern model based controller design. We chose to design a linear H_∞ controller, owing to the ability to specify requirements to the closed loop controlled system such as no steady-state error, rejection of measurement noise, and robustness against model uncertainties. These requirements have to be defined in the form of mathematical equations (weights) by which the model of the system to be controlled is extended. For this extended model a controller is calculated by minimizing the H_∞ norm[13] so that the closed loop controlled system complies with the specifications given in the controller design.

For the system identified in Sec. III a linear H_∞ controller was designed using a standard S/KS/T scheme.[13] The requirements of the closed loop system are robustness against modeling errors and as-fast-as-possible sequential control. Robustness against modeling uncertainties is necessary to account for modeling errors in the identification as well as changes in the nominal model of the AFM system, e.g., by using another cantilever. Further, integrating behavior leading to no permanent control error and robustness against modeling errors beyond 10 kHz are required because the accuracy of the identified model cannot be guaranteed at higher frequencies. The AFM system controlled by the derived controller[24] meets the required specifications. This controller is able to handle the high order dynamics of the AFM system, which makes faster image acquisition possible. In addition, changes to the nominal model that the controller is designed for, e.g., by using another cantilever, can be handled by this controller, owing to the robustness in the controller design, which means that it is no longer necessary to tune the controller after each change to the system contrary to the usage of a PID-controlled AFM system.

Figure 9 shows the comparison of a simulated step response of the closed loop controlled system using our newly derived controller and a well-tuned PID-controlled system, respectively. For a first implementation, the requirements in the design of the H_∞ controller were chosen very conservatively for the sake of robustness. Nevertheless, the comparison to the PID-controller in Fig. 9 shows a remarkable improvement of the control performance. The position of the scanner surface z settles rapidly, while the input signal of the scanner v, which was normally used to display the topographic data, still oscillates to compensate the scanner dynamics. Other simulations show that this effect is strongly reinforced by increasing the controller performance. Therefore the control signal v can no longer be used for topography acquisition. To get the current position of the scanner surface, which is the negative value of the sample's topography in the closed loop controlled AFM system, we simulated the scanner by the same mathematical model as used in the controller design (Fig. 10). The identified discrete mathematical model to simulate the scanner and a discrete state space model of the H_∞ controller are implemented on the target PC by using the Realtime Workshop of Matlab.[23]

V. EXPERIMENTAL RESULTS

To compare the performance of the H_∞ controller described above to that of the standard PID controller used by the commercial AFM, we chose to image purple membrane, 5 to 6 nm thick and several micrometer-sized patches from the plasma membrane of the Halobacterium Salinarium.[26] Purple membranes were prepared from suspension onto freshly cleaved mica substrates, allowed to adsorb for 60 s, and then rinsed in ultrahigh quality H_2O (18 MΩ cm resistivity). Images of a single patch were acquired at different scan speeds with the PID and H_∞ controller, respectively. A cantilever of the type NP Silicon Nitride Probes Nonsharpened, 200 Wide (Digital Instruments) was used.

Figures 11(a) and 11(e) and 11(b) and 11(f) show the topography and deflection signal of a purple membrane patch acquired at 20 Hz line scan rate with the H_∞ and PID controller, respectively. Figures 11(c) and 11(g) and 11(d) and 11(h) show the same area imaged at 4 Hz line scan rate with the H_∞ and PID controller, respectively. The controller error, displayed by the deflection signal which is an independent quality control, for a given scan rate is always lower for the H_∞ controller when compared to the PID controller. The average error (measured at the edges of the patch) of the H_∞ controller is 3 times and 5 times smaller than that of the PID

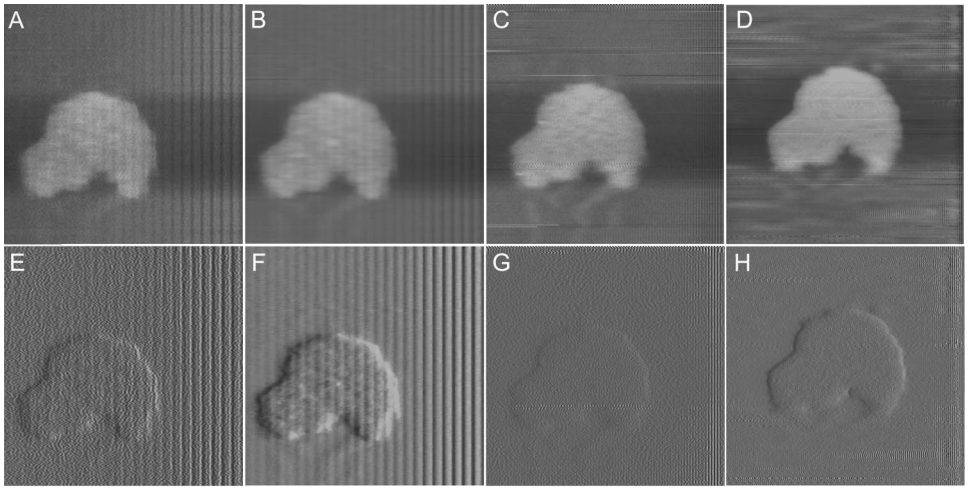

FIG. 11. Purple membrane imaged with an H_∞-controlled AFM [(a), (c), (e), and (g)] and a PID-controlled AFM [(b), (d), (f), and (h)]. All images were recorded from right to left and are 1.5 by 1.5 μm^2. The line scan rate is 20 Hz for (a), (b), (e), and (f) and 4 Hz for (c), (d), (g), and (h). The sample topography is shown in (a)–(d) [scaling from black to white is 23 nm for (a) and (c) and 25 nm for (b) and (d)]. The cantilever's deflection signal is shown in (e)–(h) [scaling is 4 nm from black to white].

controller at 20 and 4 Hz, respectively. Furthermore, in the case of the H_∞-controlled AFM a better damping of the stick slip effect occurs because of the increased controller performance. This can be seen in the image of the error signal [Fig. 11(e)] where the vertical lines are not as pronounced as for the PID-controlled AFM [Fig. 11(f)]. Other scans showed that scanning can be accomplished at weaker forces with the H_∞-controlled AFM as compared to the PID control. This is possible because the reduced deflection or error signal in the case of the H_∞ controller allows imaging closer to the minimum force value without loss of tip–sample contact.[27,28]

The H_∞ controller is designed for the complete dynamics of the closed loop AFM system and, thus, there is no need to tune the controller parameters any more (see Sec. IV).

In summary we want to emphasize that the H_∞ controller provides scanning rates which are increased by a factor of 5 compared to the PID-controlled AFM system, matching the same measurement error [compare Fig. 11(e) to Fig. 11(h)].

VI. DISCUSSION

In this article a first effort to implement a robust controller for an AFM system was made. The main interest was focused on increasing the scanning rate. A mathematical model of the AFM system was derived to design the new controller and simulate the scanner for data acquisition. The scanner has to be simulated because of persistent oscillations of the control signal which disables conventional data storage. A model based controller enables fast scanning and does not have to be tuned any more because it is designed for the complete dynamics of the AFM system. First experiments have shown that controlling the AFM by an H_∞ controller provides scanning at weaker forces and an enhancement of the scanning rate by a factor of 5 for a given deflection or error signal. This first attempt already shows a remarkable improvement. We postulate, however, that this is only a fraction of the feasible scan speed when modern control utilities are rigorously employed. Current investigations focus on this. Furthermore, a reduction of the measurement error at the edges of the sample is expected by using an observer instead of the simulation of the scanner for data storage. An observer is a control engineering tool that improves the scanner simulation by refining it with the unused information of the measured cantilever deflection. Another field of interest is to investigate the dynamic behavior of the tapping mode which seems to be nonlinear or even chaotic in several cases as shown by Basso *et al.*[29] and by our first experiments. Future work will also focus on these aspects.

ACKNOWLEDGMENTS

The authors would like to thank Dr. F. Kraus of the Automatic Control Laboratory of the Swiss Federal Institute of Technology Zürich for his help and the fruitful discussions concerning the identification of the piezo scanner.

[1] R. C. Barrett and C. F. Quate, J. Vac. Sci. Technol. B **9**, 302 (1991).
[2] H. J. Butt, P. Siedle, K. Seifert, K. Fendler, T. Seeger, E. Bamberg, A. L. Weisenhorn, K. Goldie, and A. Engel, J. Microsc. **169**, 75 (1993).
[3] S. Yumoto and N. Ookubo, Appl. Phys. A: Mater. Sci. Process. **69**, 5 (1999).
[4] R. V. Lapshin and O. V. Obyedkov, Rev. Sci. Instrum. **64**, 2883 (1993).
[5] H. J. Mamin, H. Birk, P. Wimmer, and D. Rugar, J. Appl. Phys. **75**, 161 (1994).
[6] D. Knebel, M. Amrein, K. Voigt, and R. Reichelt, Scanning **19**, 264 (1997).
[7] A. Egawa, N. Chiba, K. Homma, K. Chinone, and H. Muramatsu, J. Microsc. **194**, 325 (1999).
[8] S. R. Manalis, S. C. Minne, and C. F. Quate, Appl. Phys. Lett. **68**, 871 (1996).
[9] S. C. Minne, G. Yaralioglu, S. R. Manalis, J. D. Adams, J. Zesch, A. Atalar, and C. F. Quate, Appl. Phys. Lett. **72**, 2340 (1998).
[10] M. Ashhab, M. V. Salapaka, M. Dahleh, and I. Mezic, Automatica **35**, 1663 (1999).
[11] S. H. Hsu and L. C. Fu, *Proceedings of the IEEE International Conference on Control Applications, Kohala Coast-Island, Hawaii*, 1999 (IEEE, New York, 1999).
[12] A. Daniele, T. Nakata, L. Giarre, M. V. Salapaka, M. Dahleh, *IFAC Symposium on Robust Control Design, ROCOND 97, Budapest, Hungary* (Pergamon, Oxford, 1997).
[13] S. Skogestad and I. Postlethwaite, *Multivariable Feedback Control, Analysis and Design* (Wiley, New York, 1996).
[14] D. Sarid, *Scanning Force Microscopy* (Oxford University, New York, 1991).
[15] J. Chen, R. K. Workman, D. Sarid, and R. Höper, Nanotechnology **5**, 199 (1994).
[16] L. Ljung, *System Identification Theorie for the User*, P T R Prentice Hall Information and System Sciences Series (Prentice-Hall, Englewood Cliffs, NJ, 1987).
[17] M. Viberg, Automatica **31**, 1835 (1995).
[18] P. Van Overschee and B. De Moor, Automatica **30**, 75 (1994).
[19] E. Meyer, H. Heinzelmann, P. Grütter, Th. Jung, Th. Weisskopf, H.-R.

Hidber, R. Lapka, H. Rudin, and H.-J. Güntherodt, J. Microsc. **152**, 269 (1988).
[20] D. R. Lide, *Handbook of Chemistry and Physics*, 74th ed. (CRC, Boca Raton, FL, 1994).
[21] J. E. Sader, Rev. Sci. Instrum. **66**, 4583 (1995).
[22] St. Vinzelberg (personal communications).
[23] *Real-Time Workshop User Guide*, Matlab 5.2 (Mathworks Inc., Natick, 1997).
[24] G. Schitter, Master thesis, Institute of Robotics, ETH Zürich, Switzerland, 1999.
[25] K. J. Åström and T. Hägglund, *PID Controllers: Theory, Design, and Tuning*, 2nd ed. (Instrument Society of America, Research Triangle Park, 1995).
[26] A. E. Blaurock and W. Stoeckenius, Nature (London), New Biol. **233**, 152 (1971).
[27] A. L. Weisenhorn, P. Maivald, H.-J. Butt, and P. K. Hansma, Phys. Rev. B **45**, 11226 (1992).
[28] H. F. Knapp, *Force Curves in Atomic Force Microscopy*, edited by R. J. Colton *et al.* (Wiley, Chichester, 1998), pp. 110–112.
[29] M. Basso, L. Giarré, M. Dahleh, and I. Mezić, J. Dyn. Syst., Meas., Control **122**, 240 (2000).